Polymer Journal (2014) 46, 264–271

www.nature.com/pj

ORIGINAL ARTICLE

Aggregation and phase separation of hydrophilically modified poly(dimethylsiloxane) in methanol–water mixtures

Takashi Okuhara[1], Akihito Hashidzume, Ken Terao and Takahiro Sato

Hydrophilically modified poly(dimethylsiloxane) (HPM-PDMS) bearing quaternized amino groups on the side chains was dissolved in mixtures of methanol (MeOH) and water with a water weight fraction w_{H_2O} from 0 to 1 and with 0.1 M sodium acetate added. The degree of substitution and the degree of polymerization of this ionomer sample were 16 mol% and 1050, respectively, and the polymer concentrations were mostly $<1\%$. Although the solutions were almost transparent, they were in the two-phase region at $w_{H_2O} \geqslant 0.5$, and HPM-PDMS formed random aggregates at $w_{H_2O} < 0.5$. In the two-phase region, the coexisting concentrated phases formed colloidal particles with radii of gyration ranging from 100 to 300 nm just after dispersion. The colloidal particles, however, gradually coagulated, and the solutions became turbid when they were left standing for several days. The multiplet structure in the melt sample of HPM-PDMS may be responsible for the tentative dispersion of HPM-PDMS even in the two-phase region.
Polymer Journal (2014) **46,** 264–271; doi:10.1038/pj.2014.3; published online 26 February 2014

Keywords: aggregation; colloidal particle; hydrophilically modified poly(dimethylsiloxane); ionomer; light scattering; phase separation; small-angle X-ray scattering

INTRODUCTION

Amphiphilic polyelectrolytes are copolymers consisting of ionic and hydrophobic monomer units.[1] Their properties strongly depend on the monomer content and sequence. When these copolymers are rich in ionic monomer units, they are often referred to as hydrophobically modified polyelectrolytes, whereas copolymers rich in hydrophobic monomer units are referred to as ionomers. When we consider statistical copolymers, the former copolymers (that is, those rich in ionic monomers) are soluble or dispersible in water and often form polymer micelles in aqueous solutions.[2–8] The latter copolymers (that is, the ionomers), however, hardly dissolve in water, and their solution studies have thus far been carried out mostly in polar organic solvents.[9–15]

Poly(dimethylsiloxane) (PDMS) is a typical hydrophobic polymer that is used in release coating materials, adhesive compounds and so on. In recent years, PDMS has been modified by substitutions with various hydrophilic functional groups to impart unique solution, melt and surface properties.[16–18] Such a hydrophilically modified PDMS (HPM-PDMS) is applicable to detergents, surface modifiers, cosmetics, personal skincare products and hair conditioners, metal corrosion inhibitors, and so on.

In this study, we investigated a cationic HPM-PDMS, the chemical structure of which is depicted in Scheme 1. The cationic side groups were introduced randomly, and the degree of substitution x was 0.16. Therefore, our HPM-PDMS sample is an ionomer. Although the hydrophobicity of the PDMS main chain is strong, we found that this HPM-PDMS sample is dispersible in water, methanol (MeOH) and MeOH–water mixtures all containing 0.1 M sodium acetate (NaAc), if the polymer concentration is dilute enough. We have studied the dispersion state as well as the aggregation and phase behaviors of this sample in these solutions using light scattering and small-angle X-ray scattering (SAXS). As expected for ionomers, the dispersion state was strongly dependent on the solvent composition, which is represented in terms of the weight fraction of water w_{H_2O} in the MeOH–water mixture in this paper. The polyelectrolyte character of the ionomer was much suppressed in our ionomer solutions because of the added salt.

EXPERIMENTAL PROCEDURE

Preparation of the polymer sample and its solutions

A random copolymer sample of dimethylsiloxane and 3-chloropropylmethylsiloxane was purchased from Gelest Inc. (Morrisville, PA, USA). The content of the latter monomer was 16 mol% (determined by ^{1}H-NMR), and the degree of polymerization N_0 was 1050 (determined by static light scattering; see below). This Cl-modified PDMS sample (3.95 g including 6.5 mmol of 3-chloropropyl groups) was dissolved in 4 cm^3 of a *n*-butanol/*N*,*N*-dimethyleformamide

Department of Macromolecular Science, Osaka University, Osaka, Japan
[1]Present address: Toyobo Co. Ltd., 1-1 Katata 2-1-1, Otsu, Shiga 520-0292, Japan
Correspondence: Professor T Sato, Department of Macromolecular Science, Osaka University, 1-1 Machikaneyama-cho, Toyonaka, Osaka 560-0043, Japan.
E-mail: tsato@chem.sci.osaka-u.ac.jp
Received 25 October 2013; revised 15 December 2013; accepted 25 December 2013; published online 26 February 2014

mixture (7.5:2.5 v/v) along with 13.7 mmol of 2-dimethylaminoethanol (Wako Pure Chemical Industries, Ltd, Osaka, Japan), and the solution was heated at 110 °C for 11 h while stirring to quaternize the amino group with the chloropropyl group of the Cl-modified PDMS.[18] After evaporation of the volatile fractions, the polymer sample was recovered by reprecipitation from acetone into *n*-hexane. To remove hydrophilic low-molar-mass impurities including excess amine, the sample was dialyzed against pure water at 25 °C for a week and freeze dried. The dried waxy HPM-PDMS sample that was obtained was dissolved in a small amount of MeOH and dried in a sample vial under vacuum. From the integrated intensities of the ^{1}H-NMR peaks belonging to NCH_3 (δ 2.8 p.p.m.) and $SiCH_3$ (δ 0.2 p.p.m.), it was confirmed that all of the chloropropyl groups of the Cl-modified PDMS had reacted with 2-dimethylaminoethanol.

Light scattering and SAXS measurements were made on the HPM-PDMS sample dissolved in MeOH, water and MeOH–water mixtures, all of which included added salt to reduce strong intermolecular electrostatic interactions. To select the proper salt to be added to the HPM-PDMS solutions, solubility tests of various salts were conducted in MeOH, water and an MeOH–water mixture with the water weight fraction $w_{H_2O} = 0.5$. Solubility tests of HPM-PDMS in the three solvents with 0.1 M solutions of various salts added were also conducted. Table 1 summarizes the results of the solubility tests, in which the cation of the salts examined was sodium. Some salts did not dissolve in MeOH, and HPM-PDMS did not dissolve in MeOH or water solutions of some of the salts. On the basis of the results of these solubility tests, NaAc was selected as the added salt for our HPM-PDMS solution study.

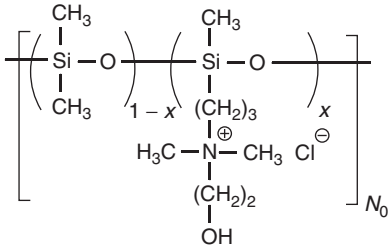

Scheme 1 Chemical structure of the hydrophilically modified poly (dimethylsiloxane) that was studied.

Table 1 Solubility tests of salts in MeOH, water and a MeOH–water mixture with $w_{H_2O} = 0.5$ as well as solubility tests of HPM-PDMS in the solvents with 0.1 M solutions of different kinds of salt added

		Solubility of salt in MeOH–water mixture			*Solubility of HPM-PDMS in 0.1 M salt solution*		
		Weight fraction of water			*Weight fraction of water*		
Cation	*Anion*	*1*	*0.5*	*0*	*1*	*0.5*	*0*
Na^+	Citrate	○	×	×	×	–	–
	Tartrate	○	×	×	×	–	–
	SO_4^{2-}	○	×	×	×	–	–
	Acetate	○	○	○	○	○	○
	Cl^-	○	○	×	○	○	–
	Br^-	○	○	○	○	○	×
	NO_3^-	○	○	×	×	○	–
	ClO_4^-	○	○	○	×	×	×
	I^-	○	○	○	×	×	×
	SCN^-	○	○	○	○	×	×
No salt		–	–	–	○	○	○

Abbreviations: HPM-PDMS, hydrophilically modified poly(dimethylsiloxane); MeOH, methanol.

The HPM-PDMS sample was directly dissolved in MeOH–water mixtures with different solvent compositions ($0 \leqslant w_{H_2O} \leqslant 1$) and containing 0.1 M NaAc and stirred by a magnetic stirrer for 24 h at room temperature. The original solutions, most of which had a polymer concentration of 1.0 wt%, were diluted with the same MeOH–water mixtures containing 0.1 M NaAc to prepare test solutions of different polymer concentrations. The test solutions were filtrated with a 0.50 μm poly(tetrafluoroethylene) membrane filter before the measurements.

Light scattering

Static and dynamic light scattering measurements were performed on the HPM-PDMS solutions at 25 °C using an ALV/SLS/DLS-5000 light scattering instrument (ALV, Langen, Germany) with a Nd:YAG laser operating at 532 nm. All the solutions were almost transparent, and light scattering measurements were carried out within 30 h after preparation. The scattered light intensity did not depend on time during the measurements.

When the solution is dilute enough, the excess Rayleigh ratio R_θ at the scattering angle θ is related to the weight-average molar mass M_w, the *z*-average particle scattering function $P(k)$ in which k is the magnitude of the scattering vector and the second virial coefficient A_2 of the solute by Yamakawa[19]

$$\frac{Kc}{R_\theta} = \frac{1}{M_w P(k)} + 2A_2 Q(k)c \tag{1}$$

where K is the optical constant, c is the polymer mass concentration, and $Q(k)$ is the intermolecular interference factor. From this equation, we have the following relations:

$$\lim_{\theta \to 0}(Kc/R_\theta)^{1/2} \equiv (Kc/R_0)^{1/2} = M_w^{-1/2} + A_2 M_w^{1/2} c \tag{2}$$

and

$$P(k)^{-1/2} = \lim_{c \to 0}\left(\frac{Kc/R_\theta}{Kc/R_0}\right)^{1/2} \tag{3}$$

Furthermore, $P(k)$ is related to the *z*-average radius of gyration $\langle S^2 \rangle_z^{1/2}$ by

$$P(k)^{-1/2} = 1 + \tfrac{1}{6}\langle S^2 \rangle_z k^2 + O(k^4) \tag{4}$$

The refractive index increment $\partial n/\partial c$ of HPM-PDMS that is needed to calculate K was determined to be 0.108 ($w_{H_2O} = 0$), 0.0869 (0.1), 0.0726 (0.3), 0.0462 (0.5), 0.0531 (0.6), 0.0579 (0.7), 0.0831 (0.9) and 0.0928 (1) $cm^3 g^{-1}$ using differential refractometry at 25 °C. These results were obtained for non-dialyzed solutions. As the refractive indices of water and MeOH are very close and because the composition dependence of the solvent refractive index is weak enough ($n^{-1}\partial n/\partial w_{H_2O}$ is $<4\%$), the preferential adsorption effect on the light scattering results was disregarded.[19]

Intensity autocorrelation functions obtained using dynamic light scattering were analyzed by the CONTIN method to obtain the hydrodynamic radius R_H.

Small-angle X-ray scattering

SAXS measurements were conducted on HPM-PDMS dissolved in MeOH–water mixtures with $w_{H_2O} = 0.5$, 0.7 and 0.9 (all including 0.1 M NaAc) at the BL40B2 beamline of SPring-8 (Hyogo, Japan, proposal no. 2012B1452). The polymer concentration was fixed to be 2×10^{-3} g cm^{-3}, and the SAXS measurements were performed on the solutions *ca* 5 days after solution preparation. The wavelength of the X-ray, the camera length and the accumulation time were set to be 0.10 nm, 3000 mm and 180 s, respectively. A capillary made of quartz that contained test solutions was set in a heating block set at 25 °C, and the intensity of the scattered X-ray was measured using an imaging plate detector. SAXS measurements were also made on the HPM-PDMS and Cl-modified PDMS samples in melt, injected into capillaries, at the BL-10C beamline in KEK-PF (Tsukuba, Japan, proposal no. 2011G557). A wavelength of 0.15 nm, a camera length of 2000 mm and an accumulation time of 100 s were chosen for this study.

RESULTS

Figure 1 shows the dependence of $(Kc/R_0)^{1/2}$ on polymer mass concentration c in MeOH–water mixtures of different solvent

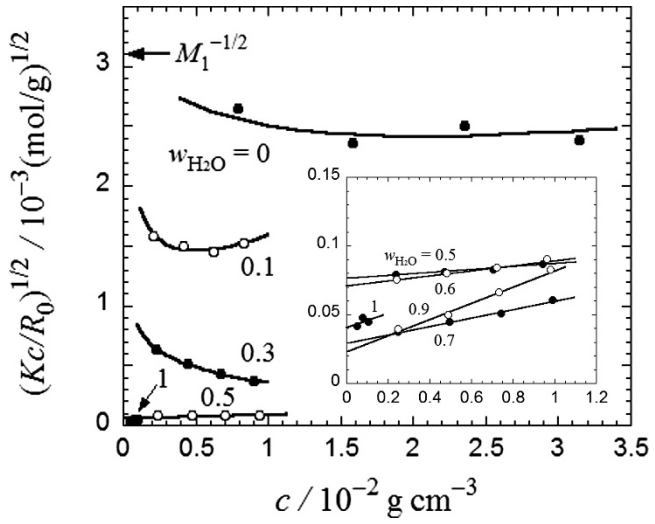

Figure 1 Dependence of $(Kc/R_0)^{1/2}$ on concentration for hydrophilically modified poly(dimethylsiloxane) (HPM-PDMS) in methanol–water mixtures with different compositions.

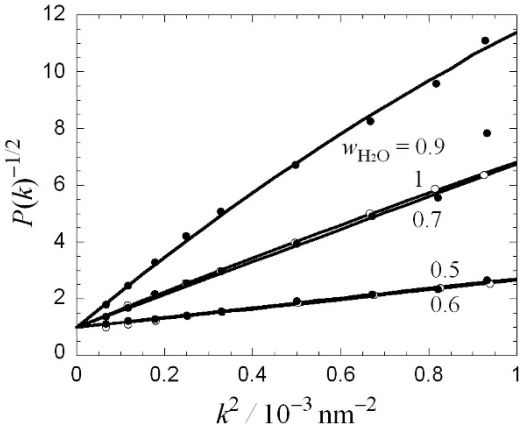

Figure 2 Particle scattering functions $P(k)$ of hydrophilically modified poly(dimethylsiloxane) (HPM-PDMS) in methanol–water mixtures with different compositions.

compositions with 0.1 M NaAc added. The data points for $w_{H_2O} = 0$ (that is, MeOH), 0.1 and 0.3 follow concave curves with negative initial slopes, and the $(Kc/R_0)^{1/2}$ values are lower than the value of $1/M_1^{1/2}$, as indicated by the arrow in the figure, where M_1 is the molecular weight of the HPM-PDMS sample. ($M_1 = 1.04 \times 10^5$, calculated from the degree of polymerization of the original Cl-modified PDMS sample). These data indicate that HPM-PDMS forms aggregates in these solvents and that the degree of aggregation increases with w_{H_2O} (*cf.* equation (2)) because of the lower affinity of the HPM-PDMS main chain with water. However, at $w_{H_2O} \geqslant 0.5$, the data points follow almost straight lines with positive slopes and very small intercepts; this demonstrates the existence of very large aggregates of HPM-PDMS in the MeOH–water mixtures.

The particle scattering functions $P(k)$ of HPM-PDMS in MeOH–water mixtures at $w_{H_2O} \geqslant 0.5$ and at infinite dilution of the polymer (*cf.* equation (3)) are shown in Figure 2. (Owing to difficulty in the concentration extrapolation, $P(k)$ were not obtained at $w_{H_2O} < 0.5$.) Strong angular dependences of $P(k)$ at $w_{H_2O} \geqslant 0.5$ also indicate the existence of large aggregates of HPM-PDMS in the MeOH–water mixtures.

From the intercepts and initial slopes of the plots shown in Figures 1 and 2, we determined the weight-average molar masses M_w, the second virial coefficients A_2 and the *z*-average root-mean-square radii of gyration $\langle S^2 \rangle_z^{1/2}$ of the HPM-PDMS aggregates in MeOH–water mixtures with $w_{H_2O} \geqslant 0.5$ (*cf.* equations (2) and (4)). The results as well as the weight-average aggregation number $m_w = M_w/M_1$ and the hydrodynamic radius R_H obtained by dynamic light scattering are listed in Table 2. The ratios $\langle S^2 \rangle_z^{1/2}/R_H$, which range from 0.9 to 1.3, are larger than that expected for the uniform density sphere, but the deviation may arise from the high dispersity in the molar masses of the aggregates, which increases the ratio.[20] If the HPM-PDMS aggregates at $w_{H_2O} \geqslant 0.5$ exist as uniform density spheres, then we can calculate the polymer mass concentration c_{in} inside the sphere using

$$c_{in} = 3M_w / 4\pi N_A R_H^3 \qquad (5)$$

The concentration c_{in} at each w_{H_2O} is listed in the last column of Table 2. The HPM-PDMS aggregate still contains much solvent.

Table 2 Characteristics of aggregates of HPM-PDMS formed in MeOH–water mixtures with $w_{H_2O} \geqslant 0.5$ that were obtained by light scattering

	$M_w/10^8$		$A_2/10^{-8}$ mol			
w_{H_2O}	g mol^{-1}	$m_w/10^3$[a]	cm^3 g^{-2}	$\langle S^2 \rangle_z^{1/2}$/nm	R_H/nm	c_{in}/g cm^{-3}[b]
0.5	1.7	1.7	8.1	100	98	0.072
0.6	2.0	1.9	14	99	110	0.059
0.7	11	11	8.9	190	150	0.14
0.9	18	18	14	280	290	0.029
1	6.3	6.1	25	190	150	0.069

Abbreviations: HPM-PDMS, hydrophilically modified poly(dimethylsiloxane); MeOH, methanol.
[a]Weight-average aggregation number estimated by M_w/M_1.
[b]Polymer mass concentration estimated by equation (5).

After the light scattering measurements were performed, the test solution of $w_{H_2O} = 0.7$ ($c = 0.01$ g cm^{-3}) was kept standing at room temperature. As shown in Figure 3, the turbidity of the solution increased slowly with time. This implies that the phase separation takes place in the solution but that the separated concentrated phase grows very slowly. However, HPM-PDMS solutions of $w_{H_2O} < 0.5$ ($c = 0.01$ g cm^{-3}) remained transparent for a long time after the solution preparation.

Figure 4 shows SAXS profiles of HPM-PDMS solutions with $w_{H_2O} = 0.5$, 0.7 and 0.9 in which the polymer concentration was fixed at 2×10^{-3} g cm^{-3}. Excess SAXS intensities $I(k)$ at $w_{H_2O} = 0.5$ are much stronger than those at $w_{H_2O} = 0.7$ and 0.9. From Guinier's plots of the $I(k)$ data at $w_{H_2O} = 0.5$ and at $0.14\ \mathrm{nm^{-1}} < k < 0.3\ \mathrm{nm^{-1}}$ (data not shown), the radii of gyration without correction of the intermolecular interference effect were estimated to be 3.2–6.5 nm, which were much smaller than that (100 nm) estimated by light scattering. If the solution contains two scattering components of extremely different sizes, then scattering from the larger component and from the smaller component is predominant in the k regions of light scattering and SAXS, respectively. Therefore, from the light scattering and SAXS data, we conclude that the solution with $w_{H_2O} = 0.5$ includes not only large aggregates but also a component of HPM-PDMS with small sizes. However, in the solutions with $w_{H_2O} = 0.7$ and 0.9, the large aggregates of HPM-PDMS that were detected by light scattering may be the predominant scattering

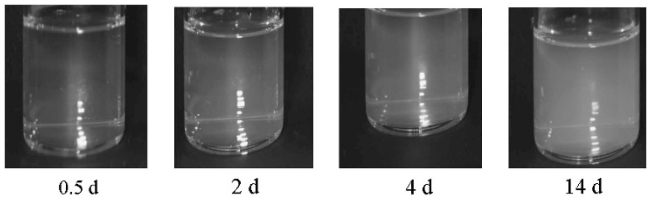

Figure 3 Appearance of the hydrophilically modified poly(dimethylsiloxane) (HPM-PDMS) solution with $w_{H_2O} = 0.7$ ($c = 0.01\,g\,cm^{-3}$) that was kept standing at room temperature at different times. A full color version of this figure is available at the *Polymer Journal* online.

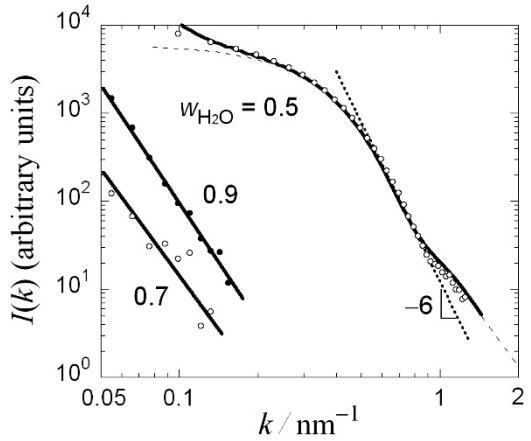

Figure 4 Small-angle X-ray scattering (SAXS) profiles of hydrophilically modified poly(dimethylsiloxane) (HPM-PDMS) in a methanol–water mixture with $w_{H_2O} = 0.5$, 0.7 and 0.9 ($c = 0.002\,g\,cm^{-3}$). The solid curve for $w_{H_2O} = 0.5$ indicates theoretical values calculated using equations (9)–(14) and the parameter values listed in Table 3, and the dashed curve for $w_{H_2O} = 0.5$ is the contribution of component S (equation (10') with $A_{SS} = 0$; see Discussion section).

component, and there is no appreciable amount of the small-size component.

DISCUSSION

Aggregation of HPM-PDMS at $w_{H_2O} \leqslant 0.3$

HPM-PDMS has a strongly hydrophobic main chain and quaternary ammonium ions on hydrophilically modified side chains. Therefore, the conformation and aggregation behavior of the HPM-PDMS chain should be determined by the balance between the hydrophobicity of the main chain and the hydrophilicity of the side chains. As demonstrated in Figure 1, HPM-PDMS forms aggregates in MeOH and MeOH–water mixtures with $w_{H_2O} = 0.1$ and 0.3 that have 0.1 M NaAc added. This aggregation may occur because of the hydrophobic main chain, but the degree of aggregation may be suppressed by the hydrophilically modified side chains.

As the hydrophobicity is uniform along the main chain of HPM-PDMS, we may not expect the formation of star-like or brush-like polymer micelles by HPM-PDMS. The flower-like micelle may also be excluded because of the difficulty in the formation of its hydrophobic core by the PDMS main chain.

Each HPM-PDMS chain in the aggregate exists as a loose coil or collapsed globule in which ammonium groups may be distributed more or less heterogeneously. In the coil or globule, sections that are poor in ammonium groups may act as binding sites to form

Table 3 List of fitting parameters for random aggregates of HPM-PDMS formed in MeOH and MeOH–water mixtures with $w_{H_2O} = 0.1$ and 0.3

w_{H_2O}	$A_2/10^{-4}$ mol cm^3 g^{-2}	f	$\Delta\varepsilon$	$\langle S^2\rangle_1^{1/2}$/nm	$c_{in,1}$/g cm^{-3} [a]
0	0.45	2.2	−3.2[b] (−3.0[c])	18	0.003
0.1	1.0	2.2	−6.5[b] (−6.8[c])	9	0.026
0.3	0	2.03	-9.8_5[b] (-9.8_5[c])	4	0.30

Abbreviations: HPM-PDMS, hydrophilically modified poly(dimethylsiloxane); MeOH, methanol.
[a]Polymer mass concentration inside the single chain forming the aggregate calculated by equation (8).
[b]Estimated by fitting data in Figure 1.
[c]Values used in the fitting of data in Figure 5.

aggregates. Here, we assume that HPM-PDMS undergoes the random aggregation in which each chain behaves on average as an f-functional unimer. For such a random aggregate, the weight-average molar mass M_w and the z-average square radius of gyration $\langle S^2\rangle_z$ can be written in the forms[5,21]

$$M_w = \frac{(1+\alpha)M_1}{1-(f-1)\alpha}, \langle S^2\rangle_z = \frac{b^2 f\alpha}{2(1+\alpha)[1-(f-1)\alpha]} + \langle S^2\rangle_1 \qquad (6)$$

where α is the reacted fraction of the functional groups and b and $\langle S^2\rangle_1$ are the distance between the nearest neighbor unimers and the square radius of gyration of the unimer, respectively, in the aggregate. Assuming the unimers in the aggregate are a uniform density sphere, we use the relation $b = 2 \times [(5/3)\langle S^2\rangle_1]^{1/2}$.

The dependence of the reacted fraction α on the polymer concentration is given by Sato and Matsuda[21]

$$\alpha = \frac{1 + 2f\phi\exp(-\Delta\varepsilon) - \sqrt{1+4f\phi\exp(-\Delta\varepsilon)}}{2f\phi\exp(-\Delta\varepsilon)} \qquad (7)$$

where ϕ is the polymer volume fraction ($\phi = c\bar{v}$ where $\bar{v}$ is the polymer partial specific volume: 0.855 cm^3 g^{-1} for PDMS) and $\Delta\varepsilon$ is the free energy change per single bond formation divided by the thermal energy. (In Sato and Matsuda,[21] $\Delta\varepsilon$ includes a concentration-dependent term, but at the dilute solutions examined in this study this term is negligible.)

Using M_w and $\langle S^2\rangle_z$ given by equation (6) as well as the second virial coefficient A_2, Kc/R_θ may be calculated using equation (1), in which the third and higher virial terms are neglected. First, we try to fit equation (2) at $k = 0$ to the experimental c dependence of $(Kc/R_0)^{1/2}$ shown in Figure 1. To do so, we need to select three parameters: f, $\Delta\varepsilon$ and A_2. As M_w must be positive, A_2 must be smaller than $(Kc/R_0)/2c$ (*cf.* equation (1)); from this equation, the maximum values of A_2 were estimated to be 9.1×10^{-5}, 1.4×10^{-4} and 8×10^{-6} mol cm^3 g^{-2} at $w_{H_2O} = 0$, 0.1 and 0.3, respectively. To obtain the best fit to the experimental c dependence of $(Kc/R_0)^{1/2}$, we had to select slightly smaller values of A_2 and then suitable values of f and $\Delta\varepsilon$. The best fit of the theoretical $(Kc/R_0)^{1/2}$ is indicated by the solid curves at $w_{H_2O} = 0$, 0.1 and 0.3 in Figure 1, and values of f, $\Delta\varepsilon$ and A_2 are listed in Table 3. The negative initial slopes of the three solid curves arise from the increase in M_w (as calculated by equation (6)) with increasing c, which is caused by the aggregation.

Furthermore, angular dependences of $(Kc/R_\theta)^{1/2}$ for solutions with $w_{H_2O} = 0$, 0.1 and 0.3, which are shown in Figure 5, are fitted to equation (1) by selecting suitable values of f, $\Delta\varepsilon$, A_2 and $\langle S^2\rangle_1^{1/2}$. The solid lines in Figure 5 are drawn using values of f, $\Delta\varepsilon$ and A_2 that are the same as or similar to those used in the fitting of Figure 1, as well as newly selected values of $\langle S^2\rangle_1^{1/2}$ (see Table 3).

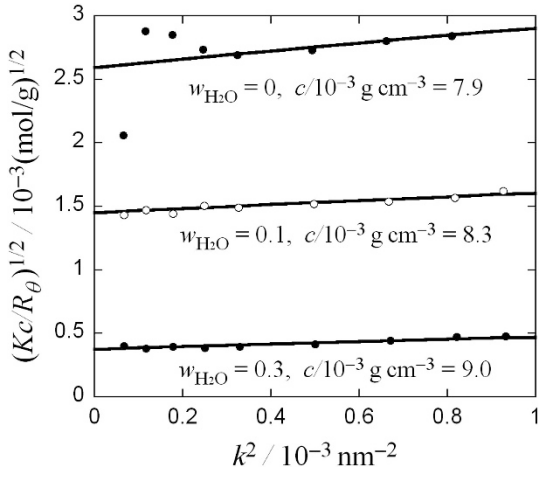

Figure 5 Angular dependence of $(Kc/R_\theta)^{1/2}$ in solutions with $w_{H_2O} = 0$, 0.1 and 0.3, used for fitting to determine the parameters characterizing the random aggregation of hydrophilically modified poly(dimethylsiloxane) (HPM-PDMS), which are listed in Table 3.

In Table 3, the absolute value of $\Delta\varepsilon$ increases and $\langle S^2\rangle_1^{1/2}$ decreases with increasing water content in the solvent. These changes occur because the intermolecular and intramolecular hydrophobic interactions of the HPM-PDMS main chain become stronger with increasing water content. As a result, the mass concentration $c_{in,1}$ inside the polymer chain forming the aggregate, which is calculated using

$$c_{in,1} = 3M_1 \Big/ 4\pi N_A \left(\tfrac{5}{3}\langle S^2\rangle_1\right)^{3/2} \tag{8}$$

increases with the water content (*cf.* the last column of Table 3). On the other hand, the f values are close to 2, indicating that the branch density of the random aggregate formed by the HPM-PDMS chains is rather low, irrespective of w_{H_2O}, which may be due to the intermolecular electrostatic repulsion. Ammonium groups may be distributed more on the periphery of the HPM-PDMS chain unimer so that the electrostatic interaction may affect A_2 in a different way than it affects $\langle S^2\rangle_1^{1/2}$.

Phase separation in the solutions at $w_{H_2O} \geqslant 0.5$

As shown in Figure 1, the light scattering behavior of dilute HPM-PDMS solutions is very different at $w_{H_2O} < 0.5$ and at $w_{H_2O} \geqslant 0.5$. The molar mass and aggregation number of the HPM-PDMS aggregates are very large at $w_{H_2O} \geqslant 0.5$ (*cf.* Table 2), implying that a liquid–liquid phase separation takes place in such dilute HPM-PDMS solutions in which the separated concentrated phase may exist as colloidal particles.

When a polymer solution of volume V and mass concentration c is demixed into dilute and concentrated phases with volumes V_d and V_c and mass concentrations c_d and c_c, respectively, we equate V_d/V and V_c/V to $(c_c - c)/(c_c - c_d)$ and $(c - c_d)/(c_c - c_d)$, respectively, using the lever rule. If the coexisting concentrated phase is dispersed as colloidal particles in the solution, there are two scattering components, the polymer component (component S) in the coexisting dilute phase and the colloidal particles of the coexisting concentrated phase (component L). The mass concentrations c_S and c_L of the components S and L, respectively, in such a phase-separated solution are given by

$$c_S = c_d \frac{V_d}{V} = c_d \frac{c_c - c}{c_c - c_d}, c_L = c_c \frac{V_c}{V} = c_c \frac{c - c_d}{c_c - c_d} \tag{9}$$

and the excess Rayleigh ratio R_θ of a solution that includes the two components is given by Sato *et al.*[22]

$$\frac{R_\theta}{Kc} = \frac{w_S M_S P_S(k) + w_L M_L P_L(k) + 2w_S w_L M_S P_S(k) M_L P_L(k)(A_{SS} + A_{LL} - 2A_{SL})c}{[1 + 2w_S M_S P_S(k) A_{SS} c][1 + 2w_L M_L P_L(k) A_{LL} c] - 4w_S w_L M_S P_S(k) M_L P_L(k)(A_{SL} c)^2} \tag{10}$$

Here, K is the optical constant, w_i, M_i and $P_i(k)$ are the weight fraction of the total polymer ($w_i = c_i/c$), the weight-average molar mass, and the z-average particle scattering function of the component i, respectively, and A_{ij} is the second virial coefficient between the components i and j (i, j = S, L).

Colloidal particles of the concentrated phase may be regarded as uniform density spheres with a log-normal distribution of the molar mass M. The particle scattering function $P_L(k)$ of the component L is then calculated using[23,24]

$$M_L P_L(k) = \int M \left[3\frac{\sin(kR_M) - kR_m \cos(kR_M)}{(kR_M)^3}\right]^2 \tfrac{1}{\sqrt{\pi}} \exp(-x^2)\, dx \tag{11}$$

where R_M is the radius of the sphere with the molar mass M, and x is defined by

$$x \equiv \sigma^{-1} \ln(M/\bar{M}) \tag{12}$$

with σ and M° being defined as

$$\sigma \equiv 2\ln(M_w/M_n), \bar{M} \equiv (M_w M_n)^{1/2} \tag{13}$$

Here, M_w and M_n are the weight-average molar mass ($M_w = M_L$) and number-average molar mass of the colloidal particles, respectively. The radius R_M is calculated using

$$R_M = \left(\frac{3M}{4\pi N_A c_c}\right)^{1/3} \tag{14}$$

If the polymer chain in the dilute phase takes a random coil conformation, $P_S(k) \propto k^{-2}$ in high k regions;[25] but the SAXS profile in Figure 4 shows a much stronger k dependence in the intermediate k region (*cf.* the dotted line with a slope of -6), which indicates that the component S exists also as spherical particles with a size dispersity. Thus, the particle scattering function $P_S(k)$ is calculated from equations (11)–(14), similarly to $P_L(k)$, but with c_c in equation (14) replaced by the concentration inside a particle of component S, $c_{in,S}$. The concentration $c_{in,S}$ may be different from c_c in the concentrated phase and may correspond to $c_{in,1}$ of the aggregate at $w_{H_2O} \leqslant 0.3$, defined by equation (8).

At high k, $P_L(k)$ diminishes to zero and we can reduce equation (10) to

$$\frac{R_\theta}{Kc} \approx \frac{w_S M_S P_S(k)}{1 + 2w_S M_S P_S(k) A_{SS} c} \text{ (at high } k) \tag{10'}$$

We determined M_S, $(M_w/M_n)_S$, and $c_{in,S}$ by fitting the SAXS data at high k to equation (10′). The thin dashed curve in Figure 4 shows the result, and the parameters chosen are listed in Table 4. As c ($= 2 \times 10^{-3}$ g cm^{-3}) was low enough, the dashed curve was not affected by the second virial term in equation (10′); w_S cannot be determined because we did not determine the absolute value of $I(k)$ in the SAXS experiment.

The dashed thin curve deviates from the experimental data only at $k < 0.2$ nm^{-1}. Thus, it is difficult to determine uniquely the parameters for component L in equation (10) from only the SAXS profile. We obtained the solid curve in Figure 4 at $w_{H_2O} = 0.5$ using the parameter values for the S and L components that are listed in Table 4 and by neglecting the virial terms (that is, $A_{SS} = A_{LL} = A_{SL} = 0$).

Table 4 Characteristics of the polymer component in the dilute phase and of colloidal particles of the concentrated phase of the HPM-PDMS solution with $w_{H_2O} = 0.5$ and $c = 0.002\,g\,cm^{-3}$ that were determined using the SAXS data shown in Figure 4

	Polymer component in the dilute phase (i=S)	Colloid particles of the concentrated phase (i=L)
M_i/g mol^{-1}	3.1×10^5	2.1×10^9
$(M_w/M_n)_i$	1.6	2.5
$c_{in,S}$[a] or c_c	$c_{in,S} = 0.53\,g\,cm^{-3}$	$c_c = 0.072\,g\,cm^{-3}$
w_i[b]	0.15	0.85
$\langle S^2 \rangle_{z,i}^{1/2}$/nm[c]	5.4	220

Abbreviations: HPM-PDMS, hydrophilically modified poly(dimethylsiloxane); SAXS, small-angle X-ray scattering.
[a]Polymer mass concentration inside the component S.
[b]Calculated from equation (9) with $c = 2 \times 10^{-3}\,g\,cm^{-3}$, $c_d = 3 \times 10^{-4}\,g\,cm^{-3}$, and $c_c = 7.2 \times 10^{-2}\,g\,cm^{-3}$.
[c]z-Average radius of gyration for the component i, calculated from the values of M_i, $(M_w/M_n)_i$, and $c_{in,S}$ or c_c.

Although the fit of the solid curve is reasonably good, the parameter values for the component L in Table 4 are not decisive. It is noted, however, that the value of c_c used to calculate w_L in Table 4 is identical with the value of c_{in} at $w_{H_2O} = 0.5$ in Table 2, which was determined from the light scattering results of M_w and R_H. (Although M_w in Table 2 is the average molar mass of components S and L, it should be close to the molar mass of component L because w_S is considerably small.)

If the HPM-PDMS solution contains the two scattering components S and L at $w_{H_2O} = 0.5$, the c dependence of $(Kc/R_0)^{1/2}$ at $w_{H_2O} = 0.5$, shown in the insert of Figure 1, as well as the experimental result of $\langle S^2 \rangle_z^{1/2} = 100$ nm at $w_{H_2O} = 0.5$ that is listed in Table 2 should be compared with equation (10) combined with equation (9). These light scattering results were reproduced using $M_L = 1.8 \times 10^8\,g\,mol^{-1}$, $(M_w/M_n)_L = 2$, $c_d = 1 \times 10^{-4}\,g\,cm^{-3}$, and $c_c = 0.1\,g\,cm^{-3}$ as well as $A_{SS} = -1.0 \times 10^{-5}$, $A_{LL} = 1.3 \times 10^{-7}$, and $A_{SL} = 1.0 \times 10^{-5}$ (in units of mol cm^3 g^{-2}), although the fitting results are not shown. As the polymer concentration and the time elapsed after solution preparation were different for the test solutions used in light scattering and in SAXS, the M_L is largely different from that listed in Table 4, but the other parameters determined by light scattering and SAXS are consistent. The solid curve in Figure 4 did not change when the A_2 values used to fit the light scattering results were substituted into equation (10).

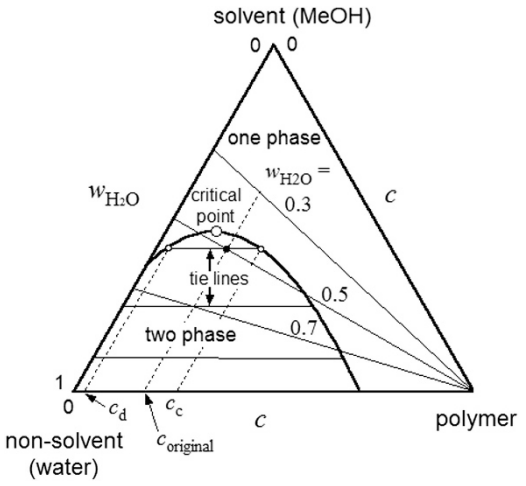

Figure 6 Schematic ternary phase diagram of a system with a polymer, solvent and non-solvent that was calculated by Tompa[26] using the Flory–Huggins theory. In the diagram, c_d and c_c indicate the polymer concentrations of coexisting dilute and concentrated phases, respectively, at $w_{H_2O} = 0.5$.

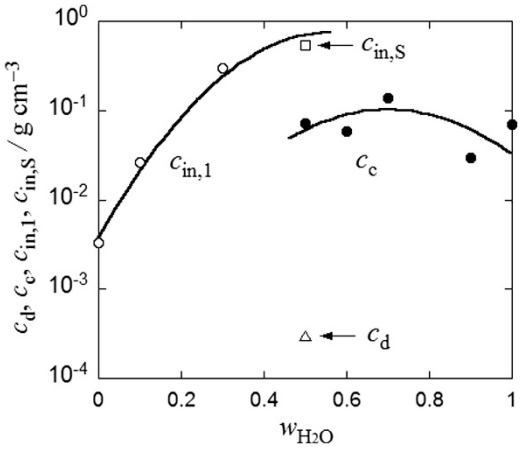

Figure 7 The dependences on solvent composition of the concentration of the coexisting concentrated phase c_c (filled circles) and the concentration inside the single polymer chain $c_{in,1}$ (unfilled circles). The polymer concentrations of the coexisting dilute phase c_d and inside the component S $c_{in,S}$ are also shown (triangle and square, respectively).

Phase diagram of the ternary system of a polymer, solvent and non-solvent

Many years ago, Tompa[26] calculated the ternary phase diagram of a system containing a polymer, solvent and non-solvent using the Flory–Huggins theory.[27] His result is schematically illustrated in Figure 6 with the composition of the ternary system specified by the polymer mass concentration c and the weight fraction w_{H_2O} of the non-solvent (that is, water) in the mixed solvent of our system. A ternary solution with the original polymer concentration $c_{original}$ is in the one-phase region of the ternary phase diagram at a low w_{H_2O} such as 0.3, but it goes into the two-phase region at a w_{H_2O} of 0.5 or 0.7. At $w_{H_2O} = 0.5$, the original solution indicated by the small filled circle in the phase diagram is separated into the dilute and concentrated phases with the polymer concentrations c_d and c_c, respectively, indicated by the two small unfilled circles in Figure 6. When w_{H_2O} increases to 0.7 and 0.9, c_d on the bimodal curve in Figure 6 becomes very dilute, which is consistent with the disappearance of the polymer component S in the SAXS profile at $w_{H_2O} = 0.7$ and 0.9.

In Table 4, the weight fraction w_S of the component S in the dilute phase is as low as 0.15 at $w_{H_2O} = 0.5$ and $c = 2 \times 10^{-3}\,g\,cm^{-3}$. We can expect an even lower w_S at $w_{H_2O} > 0.5$. Therefore, M_w, $\langle S^2 \rangle_z^{1/2}$ and R_H, which is obtained by light scattering and listed in Table 2, are regarded as good approximations of the values for component L, and c_{in} in the last column of the table can be equated with c_c of the coexisting concentrated phase. The polymer concentration c_d of the coexisting dilute phase, however, was estimated at $w_{H_2O} = 0.5$ by the combination of the SAXS and light scattering data (see above) but was not able to be estimated at $w_{H_2O} > 0.5$ because of the essential lack of contribution of component S to the SAXS profile.

Figure 7 shows the dependence of c_c on the solvent composition at $w_{H_2O} \geqslant 0.5$ (filled circles) as well as c_d at $w_{H_2O} = 0.5$ (a triangle). The filled circles at $w_{H_2O} \geqslant 0.6$ are actually the results for c_{in} listed

in Table 2, which can be equated with c_c as mentioned above. From Tompa's phase diagram (Figure 6), we can expect that c_c is a monotonically increasing function of the non-solvent composition w_{H_2O} but that c_c of our ternary system is essentially independent of w_{H_2O}. Tompa used the Flory–Huggins theory on a system in which the polymer is a non-ionic homopolymer that does not aggregate in the coexisting dilute phase and assumed the three interaction parameters in the ternary system to be constant. In our system, the intermolecular hydrophobic and electrostatic interactions among HPM-PDMS, MeOH and water should depend on the solvent composition, so the interaction parameters may not be constant. As we do not have enough information about the interaction parameters for our ternary system at present, we must postpone the discussion of the disagreement between theory and experiment that is shown in Figures 6 and 7.

At $w_{H_2O} = 0.5$, the HPM-PDMS chain (that is, component S) in the dilute phase of the phase-separated solution aggregates slightly (the aggregation number $M_S/M_1 = 3$) and takes a compact globular conformation with $c_{in,S} = 0.53\,g\,cm^{-3}$ (*cf.* Table 4). This internal concentration is higher than the concentration inside the unimer in the random aggregate that forms at $w_{H_2O} = 0$–0.3 (*cf.* Table 3 and unfilled circles in Figure 7) and almost comparable to those for globular proteins ($\approx 0.7\,g\,cm^{-3}$).[2,28] The strong hydrophobic interaction of the HPM-PDMS chain at $w_{H_2O} = 0.5$ makes $c_{in,S}$ higher.

However, the aggregation number of three of component S at $w_{H_2O} = 0.5$ is much lower than the aggregation number M_w/M_1 at $w_{H_2O} < 0.5$ that is calculated using equations (6) and (7) and the parameters listed in Table 3; for example, $M_w/M_1 = 21$ at $w_{H_2O} = 0.3$ and $c = 0.002\,g\,cm^{-3}$. In the globular state, HPM-PDMS main chains and cationic side chains may be located inside and outside the globule, respectively, as they are in globular proteins in which a ternary structure prevents random aggregation of the chains.

The globular state or the collapsed conformation of a polymer chain in a poor solvent, particularly the system of thermosensitive poly(*N*-isopropylacrylamide) in hot water, has been studied by many researchers.[29–31] However, the collapse of the polymer chain is usually accompanied by a phase separation that makes it difficult to investigate the globular state of the chain. In this study, we investigated the globular state of the HPM-PDMS chain in the phase-separated solution using SAXS such that the scattering from the concentrated phase droplets was minor because of intra-particle interference.

Dispersibility of HPM-PDMS in MeOH–water mixtures

Test solutions for light scattering and SAXS measurements were prepared by mixing the HPM-PDMS melt sample directly with MeOH–water mixtures. The dispersibility of HPM-PDMS was quite good. However, the solutions with $w_{H_2O} > 0.5$ slowly became turbid as time elapsed after dissolution (see Figure 3) and did not return to a transparent state with stirring. This means that the concentrated phase in the solutions at $w_{H_2O} > 0.5$ exists as colloidal particles just after dissolution but that the particles coagulate into larger particles and that the coagulation process is irreversible. Thus, we should discuss the origin of the dispersibility of the HPM-PDMS melt sample into MeOH–water mixtures even in the two-phase region.

We examined the bulk structure in the HPM-PDMS melt sample used for the above solution study. Figure 8 shows the SAXS profiles $I(k)$ of the melt samples of HPM-PDMS and Cl-modified PDMS before the hydrophilic modification. Although $I(k)$ for the Cl-modified PDMS is a sharply decreasing function of the magnitude of the scattering vector k, the profile for HPM-PDMS has a peak at $k = 1.27\,nm^{-1}$ that corresponds to a characteristic spacing of *ca* 5.0 nm in the melt sample. Similar SAXS peaks have been observed for many ionomers in the bulk state.[32–34] Eisenberg[35] proposed that ions of ionomers exist as multiplets in hydrophobic polymer media and look like *reverse* flower micelles or flower necklaces.[36]

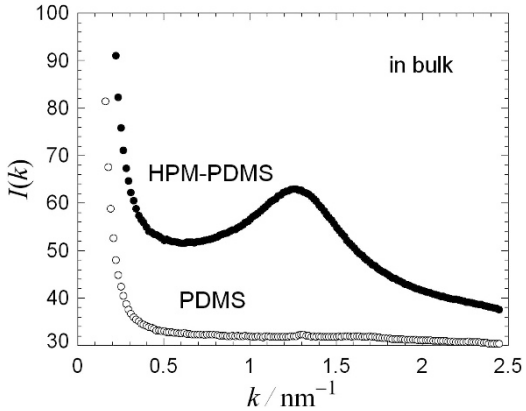

Figure 8 Small-angle X-ray scattering (SAXS) profiles of Cl-modified poly(dimethylsiloxane) (PDMS) and hydrophilically modified poly(dimethylsiloxane) (HPM-PDMS) in bulk.

When this HPM-PDMS sample is mixed with MeOH–water mixtures, the multiplet and hydrophobic polymer domains may be swollen by water and MeOH, respectively, although the swelling of the hydrophobic polymer domain is not expected at $w_{H_2O} = 1$; the swollen two-domain structure may then be destroyed by stirring to give a colloidal dispersion. As the original multiplet structure in the HPM-PDMS melt sample is nanometers in size, we expect the colloid size just after dispersion to be similar. In other words, the formation of small colloidal particles just after dissolution may reflect the nanometer-sized multiplet structure in the HPM-PDMS melt sample, as demonstrated by the SAXS profile shown in Figure 8.

The colloidal particles of the concentrated phase coagulate slowly to form larger particles. The slowness of the coagulation may be due to the electrostatic repulsion between the colloidal particles.

CONCLUSION

Dilute solutions of HPM-PDMS dissolved in MeOH–water mixtures with different water weight fractions w_{H_2O}s and with 0.1 M NaAc added were investigated using static and dynamic light scattering and SAXS. At $w_{H_2O} \leqslant 0.3$, the system is in the one-phase region, but the HPM-PDMS forms random aggregates in solution. The aggregation number increases with increasing polymer concentration and w_{H_2O}. However, at $w_{H_2O} \geqslant 0.5$, although the solutions are still transparent, they are in the liquid–liquid two-phase region. The phase behavior of the solutions qualitatively obeys the ternary phase diagram of the system of a polymer, a solvent and a non-solvent (*cf.* Figure 6), but the separated concentrated phase exists as colloidal particles of which the radius of gyration ranges from 100 to 300 nm, and the solutions maintain their transparency for several days. The SAXS profile demonstrates that the melt sample of HPM-PDMS takes on the multiplet structure of ionic groups that is often observed in ionomer samples. This nanometer-size multiplet structure may provide colloid-size droplets of the concentrated phase when the HPM-PDMS melt sample is dissolved in MeOH–water mixtures, even in the two-phase region.

ACKNOWLEDGEMENTS

We thank Professor Yo Nakamua at Kyoto University and Mr K Uramoto and M Kondo at Osaka University for helping with SAXS measurements. This work was partly supported by JSPS KAKENHI grant no. 23350055.

1 Hashidzume, A., Morishima, Y. & Szczubiałka, K. in *Handbook of Polyelectrolytes and Their Applications* (eds Tipathy, S. K., Kumar, J. & Nalwa, H.) 1–63 (American Scientific Publishers, Stevenson Ranch, CA, 2002).
2 Tominaga, Y., Mizuse, M., Hashidzume, A., Morishima, Y. & Sato, T. Flower micelle of amphiphilic random copolymers in aqueous media. *J. Phys. Chem. B* **114,** 11403–11408 (2010).
3 Mori, T., Hashidzume, A. & Sato, T. Micellization behavior of an amphiphilic statistical copolymer in water-methanol mixtures. *Polym. J.* **41,** 189–194 (2009).
4 Sato, T., Kimura, T. & Hashidzume, A. Hierarchical structures in amphiphilic random copolymer solutions. *Prog. Theor. Phys. Suppl.* **175,** 54–63 (2008).
5 Nojima, R., Sato, T., Qiu, X. & Winnik, F. M. Light scattering evidence for the random association of flower micelles of a telechelic hydrophobically-modified poly(N-isopropylacrylamide) in dilute aqueous solution. *Macromolecules* **41,** 292–294 (2008).
6 Kawata, T., Hashidzume, A. & Sato, T. Micellar structure of amphiphilic statistical copolymers bearing dodecyl hydrophobes in aqueous media. *Macromolecules* **40,** 1174–1180 (2007).
7 Nojima, R., Hashidzume, A. & Sato, T. Association–dissociation equilibrium of an amphiphilic polyelectrolyte in aqueous solution. *Macromol. Symp.* **249-250,** 502–508 (2007).
8 Hashidzume, A., Kawaguchi, A., Tagawa, A., Hyoda, K. & Sato, T. Synthesis and structural analysis of self-associating amphiphilic statistical copolymers in aqueous media. *Macromolecules* **39,** 1135–1143 (2006).
9 Marcelo, G., Mendicuti, F., Saiz, E. & Tarazona, M. P. Combination of SEC-MALS and fluorescence with molecular dynamics simulations for the analysis of ionomer dimensions in solution. application to poly(2-acrylamido-2-methyl-1-propanesulfonic acid-co-styrene). *Macromolecules* **40,** 1311–1320 (2007).
10 Nomula, S. & Cooper, S. L. Ionomer solution structure and solution diagram. *Macromolecules* **34,** 2653–2659 (2001).
11 Cirkel, P. A., Okada, T. & Kinugasa, S. Equilibrium aggregation in perfluorinated ionomer solutions. *Macromolecules* **32,** 531–533 (1999).
12 Chakrabarty, K., Seery, T. A. P. & Weiss, R. A. Characterization of ionomer solutions. 1. Phase behavior and gelation of sulfonated polystyrene ionomers in decalin. *Macromolecules* **31,** 7385–7389 (1998).
13 Lantman, C. W., MacKnight, W. J., Peiffer, D. G., Sinha, S. K. & Lundberg, R. D. Light scattering studies of ionomer solutions. *Macromolecules* **20,** 1096–1101 (1987).
14 Hara, M. & Wu, J.-L. Low-angle light scattering study of polyelectrolyte behavior of ionomers in polar solvent. *Macromolecules* **19,** 2887–2888 (1986).
15 Lundberg, R. D. & Makowski, H. S. Solution behavior of ionomers. i. metal sulfonate ionomers in mixed solvents. *J. Polym. Sci.: Polym. Phys. Ed.* **18,** 1821–1836 (1980).
16 Fortuniak, W., Chojnowski, J. & Sauvet, G. Controlled synthesis of siloxane polymers and siloxane-siloxane block copolymers with 3-chloropropyl groups pendant to the siloxane chain. *Macromol. Chem. Phys.* **202,** 2306–2313 (2001).
17 Sauvet, G., Fortuniak, W., Kazmierski, K. & Chojnowski, J. Amphiphilic block and statistical siloxane copolymers with antimicrobial activity. *J. Polym. Sci.: Part A: Polym. Chem* **41,** 2939–2948 (2003).
18 Fortuniak, W., Rözga-Wijas, K., Chojnowski, J., Labadensb, F. & Sauvet, G. Reactions of tertiary hydroxyalkylamines with 3-halogenopropyl substituted polysiloxanes: a route to water soluble and amphiphilic silicones. *Reactive Functional Polym* **61,** 315–323 (2005).
19 Yamakawa, H. *Modern Theory of Polymer Solutions* (ed. Rice, S. A.) (Harper & Row, New York, 1971).
20 Kanao, M., Matsuda, Y. & Sato, T. Characterization of polymer solutions containing a small amount of aggregates by static and dynamic light scattering. *Macromolecules* **36,** 2093–2102 (2003).
21 Sato, T. & Matsuda, Y. Macromolecular assemblies in solution: characterization by light scattering. *Polym. J.* **41,** 241–251 (2009).
22 Sato, T., Jinbo, Y. & Teramoto, A. Light scattering study of semiflexible polymer solutions III. Multicomponent solutions. *Polym. J.* **31,** 285–292 (1999).
23 Takahashi, R., Sato, T., Terao, K., Qiu, X.-P. & Winnik, F. M. Self-Association of a thermosensitive poly(2-oxazoline) block copolymer in aqueous solution. *Macromolecules* **45,** 6111–6119 (2012).
24 Sato, T., Tanaka, K., Toyokura, A., Mori, R., Takahashi, R., Terao, K. & Yusa, S.-i. Self-association of a thermosensitive amphiphilic block copolymer poly(*n*-isopropylacrylamide)-*b*-poly(*n*-vinyl-2-pyrrolidone) in aqueous solution upon heating. *Macromolecules* **46,** 226–235 (2013).
25 Kirste, R. G. & Oberthur, R. C. in *Small Angle X-ray Scattering* (eds Glatter, O. & Kratky, O.) 387–431 (Academic Press, London, 1982).
26 Tompa, H. Phase relationship in polymer solutions. *Trans. Faraday Soc.* **45,** 1142–1152 (1949).
27 Flory, P. J. *Principles of Polymer Chemistry* (Cornell Univ. Press, Ithaca, New York, 1953).
28 Tanford, C. *Physical Chemistry of Macromolecules* (John Wiley & Sons, New York & London, 1961).
29 Wu, C. & Zhou, S. Thermodynamically stable globule state of a single poly (*n*-isopropylacry1amide) chain in water. *Macromolecules* **28,** 5388–5390 (1995).
30 Wang, X., Qiu, X.-P. & Wu, C. Comparison of the coil-to-globule and the globule-to-coil transitions of a single poly(n-isopropylacrylamide) homopolymer chain in water. *Macromolecules* **31,** 2972–2976 (1998).
31 Maki, Y. & Dobashi, T. Comparison of the kinetics of chain aggregation and chain collapse in dilute polymer solutions. *Phys. Rev. E* **78,** 041802 (2008).
32 Delf, B. W. & MacKnight, W. J. Low angle X-ray scattering from ethylene-methacrylic acid copolymers and their salts. *Macromolecules* **2,** 309–310 (1969).
33 Yarusso, D. J. & Cooper, S. L. Microstructure of ionomers: interpretation of small-angle x-ray scattering data. *Macromolecules* **16,** 1871–1880 (1983).
34 Galambos, A. F., Stockton, W. B., Koberstein, J. T., Sen, A., Weiss, R. A. & Russell, T. P. Observation of cluster formation in an ionomer. *Macromolecules* **20,** 3091–3094 (1987).
35 Eisenberg, A. Clustering of ions in organic polymers. A theoretical approach. *Macromolecules* **3,** 147–154 (1970).
36 Ueda, M., Hashidzume, A. & Sato, T. Unicore-multicore transition of the micelle formed by an amphiphilic alternating copolymer in aqueous media by changing molecular weight. *Macromolecules* **44,** 2970–2977 (2011).